Environmental Science and Pollution Research (2023) 30:943–955
https://doi.org/10.1007/s11356-022-21797-4

RESEARCH ARTICLE

Silicon reduces zinc absorption and triggers oxidative tolerance processes without impacting growth in young plants of hemp (*Cannabis sativa* L.)

Marie Luyckx[1] · Jean-François Hausman[2] · Gea Guerriero[2] · Stanley Lutts[1]

Received: 9 March 2022 / Accepted: 28 June 2022 / Published online: 30 July 2022

Abstract
Hemp (*Cannabis sativa* L.) is a promising crop for non-food agricultural production on soils contaminated by moderate doses of heavy metals, while silicon, as a beneficial element, is frequently reported to improve stressed plant behavior. Using a hydroponic system, plants of *Cannabis sativa* (cv. Santhica 27) were exposed for 1 week to 100 µM Zn in the presence or absence of 2 mM Si. Zinc accumulated in all plant organs but was mainly sequestered in the roots. Additional Si reduced Zn absorption but had no impact on Zn translocation. Zn accumulation had a slight negative impact on leaf number, stem length, and chlorophyll content, and additional Si did not mitigate these symptoms. Exogenous Si reduced the Zn-induced membrane lipid peroxidation (assessed by malondialdehyde quantification) and increased the total antioxidant activities estimated by the FRAP index. In the absence of Si, leaf phytochelatin and total glutathione were the highest in Zn-treated plants and Si significantly decreased their concentrations.

Keywords *Cannabis sativa* · Hemp · Phytoremediation · Silicon · Zinc

Introduction

Increasing numbers of agriculturally used areas are contaminated by anthropogenic-derived heavy metals (HM) (Ali et al. 2013; Linger et al. 2002). Management of these areas constitutes a major environmental challenge since toxic elements absorbed by cultivated plants may contaminate the food chain and represent a major risk for human health (Linger et al. 2002; Muthusaravanan et al. 2018). These areas are therefore no longer suitable for food crop production. Other crop species may be used for bioenergy production but considering HM phytotoxicity, resistance mechanisms have to set up to mitigate their deleterious impacts on plant metabolism. Moreover, the repair of toxic-associated damages consumes metabolic energy which cannot be affected for growing processes and this often leads to a decrease in biomass production (Kim et al. 2017; Shahid et al. 2019). Consequently, the costs associated with environmental pollution are potentially enormous (Etesami and Jeong 2018).

Several approaches exist to reduce soil pollution. Phytoremediation, based on the ability of plants to extract, degrade, or immobilize various contaminants from polluted soils, appears as an interesting and ecologically friendly alternative to the traditional remediation strategies (Kurade et al. 2021). However, it still faces some limitations: HM hyper-accumulating plants are able to accumulate high concentrations of toxic elements in their aboveground parts but clean up only the soil surface because of their shallow root systems. Moreover, they produce low shoot biomass, so that the amounts of elements extracted from the soil remain extremely low (Khan et al. 2000; Muthusaravanan et al. 2018). The possibility of combining phytoremediation and non-food production, with the view of achieving low-price decontamination of soil by the production of a commercially usable resource, arouses more and more interest

Responsible Editor: Gangrong Shi

✉ Marie Luyckx
marie.luyckx@uclouvain.be

[1] Groupe de Recherche en Physiologie végétale, Earth and Life Institute – Agronomy (ELIA), Université Catholique de Louvain, 5 (Bte13) Place Croix du Sud, 1348 Louvain-la-Neuve, Belgium

[2] Environmental Research and Innovation (ERIN) Department, Luxembourg Institute of Science and Technology (LIST), 5 Avenue des Hauts-Fourneaux, 4362 Esch/Alzette, Luxembourg

(Vareda et al. 2019; Kanwar et al. 2020; Kurade et al. 2021). The implementation of this strategy requires the selection of fast-growing crops with high HM uptake and tolerance mechanisms to accumulated HM. Among plants producing a high aboveground biomass and a deep root system, *Cannabis sativa* is a multi-purpose promising crop widely employed in many types of non-food industries (Citterio et al. 2003; Schluttenhofer and Yuan 2017; Yang et al. 2020; Zhao et al. 2020). The plant indeed provides cortical fiber mainly used in paper industry and for manufacture of various products (composites, insulators, reinforced thermoplastics), while hurds present in the central part of the stem are used as animal litter and for building materials such as hempcrete (Deleuran and Flengmark 2006). Hemp would also be able, to a certain extent, to reduce Cu, Cd, and Pb contamination in polluted soils, making it a good candidate for soil phytoremediation (Angelova et al. 2004; Bona et al. 2007; Shi et al. 2009 and 2012; Ahmad et al. 2016; Kumar et al. 2017; Wu et al. 2021).

Zinc is an essential element for all living organisms and it assumes key biological functions during plant growth and development, acting as a cofactor for numerous enzymes and being integrated in the electron transport chain within mitochondria and chloroplasts (Zlobin 2021). The natural origin of zinc in soils comes from a chemical and physical degradation of the parent rock. The lithosphere typically contains between 70 and 80 mg of Zn per gram of soil, while the sedimentary rocks contain 10–120 µg g^{-1} Zn (Sun et al. 2022). Although Zn occurs naturally, it could also be inadvertently introduced to soils through anthropogenic activities such as mining, metallurgical and petrochemical industries, fertilizers, and pesticides leading to toxic accumulation of this element (Liu et al. 2018; Luo et al. 2022). In Europe, approximately 137,000 km^2 of agricultural lands have been estimated to be contaminated by HM to a certain degree, among which Zn is by far the most abundant (Tóth et al. 2016).

Zinc excess has a detrimental effect on plant growth (Zlobin 2021). It affects the plant water status and compromises photosynthesis through a decrease in pigment concentration and reduce stomatal conductance, and it alters respiration and nitrogen metabolism (Cambrollé et al. 2013; Emamverdian et al. 2015; Luyckx et al. 2019). It was also reported to affect absorption and translocation of other essential elements. Zinc toxicity damages not only the membranes and proteins but also the genetic material through association with phosphate group of DNA (Andrejić et al. 2018; Bokor et al. 2014; Zlobin 2021). Although Zn is a non-redox heavy metal, overgeneration of reactive oxygen species (ROS) may be possible due to metabolic disturbances in numerous metabolic pathways. In order to cope with oxidative stress, plants may produce antioxidant molecules among which glutathione plays a key role (Goodarzi et al. 2020). Moreover, glutathione acts as a precursor of phytochelatins which are cysteine rich peptides able to bind HM and sequester those complexes in the vacuole avoiding the toxic effects of free HM in cytosol and organels (Fan et al. 2018; Tennstedt et al. 2009). Growth inhibition occurring in Zn-treated plants may be regarded as the ultimate consequence of modifications in numerous physiological properties but other modifications may occur after plant growth inhibition occurs. Hence, analyzing the plant behavior before growth inhibition occurs may help us to identify the key properties responsible for such subsequent growth decrease.

To enhance crop growth and help the plant to cope with HM toxicity, the use of silicon (Si)-fertilizer is predicted to become a sustainable strategy and constitutes an emerging trend in agriculture (Etesami and Jeong 2018). Silicon is a non-essential element but it can contribute to improve the behavior of plant exposed to wide range of environmental constraints, including HM (Doncheva et al. 2009; Adrees et al. 2015; Imtiaz et al. 2016; Etesami and Jeong 2018). As far as hemp is concerned, Si was shown to mitigate the deleterious effect of salt (Berni et al. 2021) and Cd (Luyckx et al. 2021a) toxicities, but Si impact on Zn-exposed plants requires additional experiments. Si can also accumulate within the parietal structures where it is present in the form of orthosilicic acid and contribute to reinforce the mechanical properties of the cell wall polymers (Kröger and Poulsen 2008). As far as hemp fibers are concerned, silica treatments after harvest also provide technical advantages such as moisture buffering properties or acting as a fire retardant (Branda et al. 2016; Jiang et al. 2018).

The present work was therefore undertaken in order to evaluate the impact of a toxic dose of Zn on *Cannabis sativa* cultivated in the presence or absence of exogenous Si. Zn accumulation was quantified in different plant organs. The impacts of toxic ions on mineral nutrition, photosynthesis, and oxidative stress were recorded before growth inhibition occurs in order to identify physiological properties involved in early response of plant to Zn stress.

Material and methods

Plant material and growing conditions

Seeds of a monoecious hemp fiber cultivar (*Cannabis sativa* cv. Santhica 27) were sown in loam substrate in greenhouse conditions. After 1 week, the obtained seedlings were transferred to nutrient Hoagland solution (in mM: 2.0 KNO_3, 1.7 $Ca(NO_3)_2$, 1.0 KH_2PO_4, 0.5 NH_4NO_3, 0.5 $MgSO_4$, 17.8 Na_2SO_4, 11.3 H_3BO_3, 1.6 $MnSO_4$, 1 $ZnSO_4$, 0.3 $CuSO_4$, 0.03 $(NH_4)_6Mo_7O_{24}$, and 14.5 Fe-EDDHA) in 5-L tanks: for each tank, the seedling was adapted to plugged hole in

a polystyrene plate floating at the top of the solution. Tanks were placed in a phytotron under fully controlled environmental conditions (constant temperature of 24 ± 1 °C with a mean light intensity of 230 µmoles m^{-2} s^{-1} provided by Philips lamps (Philips Lighting S.A., Brussels, Belgium) (HPI-T 400 W), a photoperiod of 16 h under a relative humidity of 65%). After a week of acclimatization, half of the tanks received Si in the form of H_2SiO_3 to a final concentration of 2 mM Si. Metasilicic acid was obtained from a pentahydrate sodium metasilicate ($Na_2SiO_3 \times 5\ H_2O$) which was passed through an H^+ ion exchanger resin IR 20 Amberlite type according to Dufey et al. (2014). Tanks were randomly arranged in the phytotron and nutrient solution was permanently aerated by SuperFish Air Flow 4 pump. A week later, Zn was applied in the form of $ZnCl_2$ (100 µM). The Zn and Si concentrations were chosen on the basis of our previous work (Luyckx al. 2021b). The pH of the solution was maintained at 5.5. Solubility of added Zn was confirmed by the Visual MINTEQ09 software. Four treatments were thus defined, considering the presence of Zn and the concomitant presence or absence of Si and will be hereafter designed as C (control: no heavy metals and no Si), CSi, Zn, and ZnSi (7 tanks per treatment).

Harvests were performed after a week of Zn exposure. Stem length and diameter, number of leaves, and main root length were considered. Roots were quickly rinsed in deionized water for 30 s under gentle agitation just before harvest to remove ions from the free spaces: roots, stems, and leaves were then separated. Roots and leaves from a same treatment were pooled, quickly frozen in liquid nitrogen and then stored at − 80 °C until analysis, except subsamples of 3 plants per treatment incubated in an oven at 70 °C for 72 h to estimate dry weight and water content and to determine ion content.

Physiological measurements

Before plant harvest, physiological measurements were performed on 5 plants per treatment, on the middle portion of the leaf blades constituting the second fully formed leaf from the top. Chlorophyll fluorescence was measured using a fluorescence monitoring system (Hansatech Instruments). Leaf portions were dark-adapted for at least 30 min. A saturation pulse (18,000 µmol m^{-2} s^{-1}) was then sent to the leaf. The leaf was subsequently exposed to a constant intensity of actinic light (600 µmol m^{-2} s^{-1}) for 3 min, followed by a second saturating pulse of 18,000 µmol m^{-2} s^{-1}. Maximum quantum yield of dark acclimated leaves (F_v/F_m), photosystem II efficiency (Φ_{PSII}), non-photochemical quenching (NPQ), and photochemical quenching (q_P) was estimated according to Maxwell and Johnson (2000).

Leaf stomatal conductance (g_s) was measured using an AP4 diffusion porometer (Delta-TDevices Ltd., Cambridge, UK). The instantaneous CO_2 assimilation under ambient conditions (400 ppm CO_2) (*A*) and instantaneous transpiration (*E*) was measured using an infrared gas analyzer (LCA4 8.7 ADC, Bioscience, Hertfordshire, UK) with a PLC Parkinson leaf cuvette on intact leaves for 1 min (20 records min^{-1}) and an air flow of 3 mL min^{-1}. All measurements were performed between 12 a.m. and 2 p.m. The total chlorophyll (a + b) and carotenoid concentrations were measured according to Lichtenthaler (1987): 100 mg ground fresh samples was homogenized in 10 mL of cold acetone then centrifuged at 936 g for 10 min at 4 °C. Absorbance was measured on supernatant at 663.2 nm, 646.8 nm, and 470 nm.

For osmotic potential determination (Ψs), the middle portion of the leaf blades constituting the second fully formed leaves from the top was quickly collected from five plants, placed in Eppendorf tubes perforated with small holes, and immediately frozen in liquid nitrogen. Samples were then thawed 5 min at ambient temperature to rupture the membranes. Freeze-thawing cycles were repeated three times. Then, each tube was then encased in a second intact Eppendorf tube and centrifuged at 8000 g for 15 min at 4 °C. The osmolarity of the collected sap was analyzed with a vapor pressure osmometer (VAPRO® Vapor Pressure Osmometer 5520).

Mineral concentration

Fresh matter was dried in an oven for at least 48 h until it reaches a constant weight: 50–100 mg dry matter (DM) was then digested in 68% HNO_3 and acid evaporated to dryness on a sand bath at 80 °C. Minerals were incubated with a mix of HCl 37% HNO_3 68% (3:1) and the mixture was slightly evaporated and dissolved in distilled water. After filtration on Whatman no. 1 filter papers, cations and sulfur were quantified by inductively coupled plasma-optical emission spectroscopy (Varian, type MPX). For Si quantification, 1 g DM was placed in an oven and heated to 500 °C for 48 h. Ashes were then mixed with 0.4 g tetraborate and 1.6 g metaborate and heated to 1000 °C for 5 min. The obtained pellet was dissolved with 34% HNO_3. Cations were quantified by inductively coupled plasma-optical emission spectroscopy (Varian, type MPX).

Translocation factor reflects the capacity of the plant to translocate HM from the root to the shoot and was estimatsed according to Luyckx et al. (2021a) (i) on the basis of the concentration expressed on a dry weight basis in each plant part (TF_c) and (ii) on the basis of the total amount of the considered element (TF_a).

TF_c Zn concentration in the shoot/Zn concentration in the root.

TF_a Total Zn amount accumulated in the shoot / Zn accumulated in the root.

The bioaccumulation factor (BF) considers the capacity of the plant to store heavy metals in relation to external concentration. Since a nutrient solution was used in the present work rather than a solid substrate, the Zn internal concentration in the plant was estimated on a water content basis, considering the proportion of the different organs:

BF Zn concentration in the plant (mg·L−1)/Zn concentration in the solution (mg·L−1).

Malondialdehyde (MDA) content and total antioxidant activities

The level of lipid peroxidation in the control and Zn-treated plants was assessed from the concentration of malondialdehyde (MDA) as determined by the thiobarbituric acid (TBA) reaction (Heath and Packer 1968): 0.25 g of ground fresh samples was homogenized in 5 mL of 5% (w/v) trichloroacetic acid (TCA) containing 1.25% glycerol. The homogenate was centrifuged (Sigma 3–30 K, Germany) at 12,000 g for 10 min at 4 °C and filtered on Whatman no. 1 filter paper. Two milliliters of TBA (0.67%) was added to 2 mL of supernatant and the mixture was heated at 100 °C for 30 min. The reaction was stopped by placing the reaction tubes in an ice bath. The samples were centrifuged at 12,000 g for 1 min and their absorbance was measured at 532 nm (UV-1800 Shimadzu, Belgium). The results were corrected by subtracting the non-specific absorbance component as measured at 600 nm. The concentration of MDA (nmol g^{-1} DW) was calculated using an extinction coefficient of 155 mM^{-1} cm^{-1}.

To estimate the total global antioxidant activity, ferric reducing ability of plasma (FRAP) was assayed according to Benzie and Strain (1996) considering the ability of plant extract to reduce ferric to ferrous ions at low pH and to produce a colored ferrous-tripyridyltriazine complex which was spectrophotometrically detected at 593 nm: 1 g FM was frozen in liquid nitrogen, ground in the presence of 10 mL methanol, incubated during 12 h at 4 °C, and then centrifuged during 20 min at 10,000 g at 4 °C (Sigma 3–30 K, Germany). Supernatant containing the hydrophilic fraction (AOAM) was stored at − 20 °C until analysis. Pellets were dissolved in 10 mL dichloromethane, homogenized and incubated at 4 °C during 12 h, and centrifuged again at 10,000 g during 20 min (Sigma–30 K, Germany). The obtained supernatant corresponds to the hydrophobic fraction (AOAD) and was stored at − 20 °C. For the final analysis, 150 µL of each fraction was separately added to 300 µL of freshly prepared FRAP reagent (25 mL acetate buffer pH 3.6, 2.5 mL of 2,4,6-tripyridyl-s-triazine, and 2.5 mL $FeCl_3.6H_2O$ 20 mM). Standard curve was established with Trolox (50–800 µM). The concentration was expressed in µM of trolox equivalents (TE) g^{-1} of fresh material.

Glutathione and total non-protein thiols

For the reduced (GSH) and total (GSHt) glutathione quantification, 200 mg of frozen samples was extracted and derivatized by orthophthalaldehyde (OPA) according to Cereser et al. (2001). GSHt was quantified after a reduction step of oxidized glutathione (GSSG) by dithiotreitol. Extracts were filtered through 0.45-µm microfilters (Chromafil PES-45/15, Macherey–Nagel) prior to injection and OPA derivatives were separated on a reversed-phase HPLC column with an acetonitrile-sodium acetate gradient system and detected fluorimetrically. Five microliters of sample was injected into a Shimadzu HPLC system (Shimadzu, 's-Hertogenbosch, The Netherlands) equipped with a Nucleodur C18 Pyramid column (125×4.6 mm internal diameter; 5 µm particle size) (Macherey–Nagel, Duren, Germany). Derivatives were eluted in acetonitril gradient in a 50 mM sodium acetate buffer pH 6.2 at 30 °C at a flow rate of 0.7 mL min^{-1}. Fluorimetric detection was performed with a spectra system Shimadzu RF-20A fluorescence detector at 420 nm after excitation at 340 nm. GSH was quantified using nine-point calibration curves with custom-made external standard solutions ranging from 0.0625 to 50 µM and every ten injections, a check standard solution was used to confirm the calibration of the system. The recovery was determined using GSH as an internal standard. The total non-protein thiol (NPT) concentration was determined according to De Vos et al. (1992): 200 mg FM of tissue was ground in 2 mL of 5% (*w/v*) sulfosalicylic acid plus 6.3 mM diethylenetriaminepentaacetic acid (pH < 1) at 0 °C with quartz sand in a mortar. The homogenate was centrifuged at 10,000 g for 10 min at 4 °C (Sigma 3–30 K, Germany). The supernatants were collected and used for the determination of thiols using Ellman's reagent. Three hundred microliters of supernatant was mixed with 630 µL of 0.5 M KH_2PO_4 and 25 µL of 10 mM 5,5-dithiobis 2-nitrobenzoic acid (final pH 7.0). The absorbance at 412 nm was recorded after 2 min, and the NPT concentration was estimated using an extinction coefficient of 13,600 M^{-1} cm^{-1}. Phytochelatin content was evaluated as difference between NPT and GSH levels (Schäfer et al. 1997).

Statistical analysis

All analysis were performed on 5 replicates. Normality of the data was verified using Shapiro–Wilk tests and the data were transformed when required. Two-way ANOVA were

performed at a significant level of P-value < 0.05 using R (version 3.3.1) considering the Zn and the Si applications as main factors. Means were compared using Tukey's HSD all-pairwise comparisons at 5% level as a post-hoc test.

Results

Plant growth

Zinc excess induced leaf chlorosis and early senescence marked by a wilting process, especially in the youngest leaves (Fig. 1). The used hemp cultivar exhibited a high level of variability for Zn response. Despite obvious injury symptoms, Zn had no significant impact on leaf and stem dry weights (Table 1), stem diameter, and main root length (Fig. 2) but it significantly reduced the total leaf number and mean stem length (Fig. 2).

Silicon addition to control nutrient did not impact plant behavior in terms of growth or morphological properties. Silicon did not afford obvious protection against Zn toxicity and ZnSi was even the most deleterious treatment for root growth (Table 1).

Mineral concentrations

Zinc significantly accumulated in response to 100 µM $ZnCl_2$ in all plant organs. Zn was mainly accumulated in roots followed

Fig. 1 *Cannabis sativa* plants cultivated in hydroponic conditions; C: control plants; Zn: plants exposed for 1 week to 100 µM Zn

Table 1 Fresh weight (FW), dry weight (DW), water content (WC), and osmotic potential (Ψ_s) of *Cannabis sativa* (cv. Santhica 27)

	C	CSi	Zn	ZnSi
FW (g)				
Roots	11.88 ± 11.31 *a*	8.93 ± 7.54 *ab*	6.04 ± 3.59 *ab*	3.97 ± 3.02 *b*
Stems	10.03 ± 3.49 *a*	9.09 ± 5.00 *a*	4.19 ± 3.04 *b*	4.83 ± 2.94 *b*
Leaves	19.67 ± 9.37 *a*	18.20 ± 10.66 *ab*	10.59 ± 4.96 *bc*	9.45 ± 4.10 *c*
DW (g)				
Roots	0.87 ± 0.19 *ab*	0.95 ± 0.25 *a*	0.57 ± 0.20 *bc*	0.48 ± 0.16 *c*
Stems	1.22 ± 0.28 *a*	1.27 ± 0.23 *a*	0.71 ± 0.41 *a*	1.00 ± 0.47 *a*
Leaves	3.40 ± 1.58 *ab*	3.97 ± 0.83 *a*	2.40 ± 1.03 *ab*	2.09 ± 0.65 *b*
WC (%)				
Roots	88.05 ± 8.00 *a*	94.28 ± 0.58 *a*	92.54 ± 1.26 *a*	91.53 ± 1.68 *a*
Stems	86.17 ± 3.16 *ab*	90.92 ± 0.58 *a*	89.22 ± 2.01 *ab*	86.18 ± 2.42 *b*
Leaves	82.12 ± 2.36 *a*	85.54 ± 1.38 *a*	82.49 ± 2.33 *a*	82.01 ± 3.45 *a*
Ψs (Mpa)				
Leaves	− 1.21 ± 0.06 *a*	− 1.18 ± 0.04 *a*	− 1.34 ± 0.04 *b*	− 1.19 ± 0.04 *a*

Plants were exposed for 1 week to Zn (100 µM) in the presence or in the absence of 2 mM H_2SiO_3. For a given organ, different letters indicate significant differences at $P < 0.05$ according to Tukey's HSD all-pairwise comparisons. Each value is the mean of 3 replicates (FW, DW, and WC) or 5 replicates (Ψ_s)

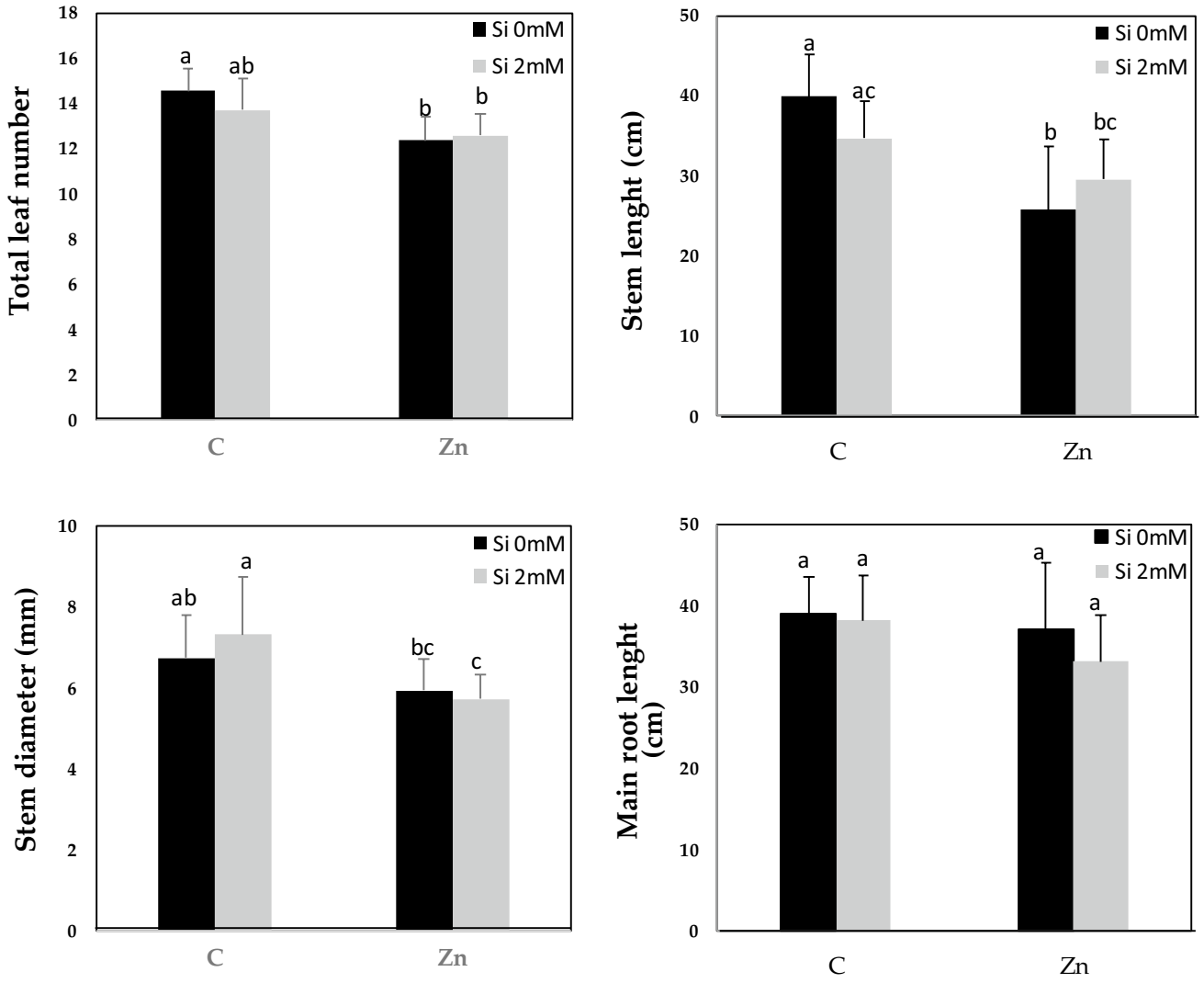

Fig. 2 Total leaf number, stem length and diameter, and root length of *Cannabis sativa* (cv. Santhica 27) exposed for 1 week to Zn (100 µM), in the presence or in the absence of 2 mM H_2SiO_3. Data are means ± standard errors ($n = 5$). Values with different letters are significantly different ($P < 0.05$; Tukey's HSD all-pairwise comparisons)

by stems and leaves (Table 2). In the absence of Zn stress, H_2SiO_3 application had no impact on Zn content. In the presence of Zn excess, however, exogenous Si significantly reduced Zn accumulation in all organs. Both TF_c and TF_a for Zn increased in response to exogenous Si in the absence of Zn excess, while BF values significantly decreased. Zn excess reduced TF_c and TF_a values and in this case, Si had no impact anymore on translocation factors or BF values.

Although not intentionally added to the nutrient solution, Si was detected in control plants probably as a consequence of the presence of Si traces in the salt used for nutrient solution preparation. Root Si increased in response to H_2SiO_3 application and the recorded increase was by far higher in Zn-treated plants than in control ones. In contrast, only a slight effect of exogenous Si on Si content was recorded in the stem which remained low comparatively to other organs. In response to H_2SiO_3 application, the leaves displayed a higher Si concentration than the stem, and the leaf Si concentration was higher in the absence of Zn excess than in the presence of high Zn concentration. In the absence of additional exogenous Si, the Si concentration in the roots and in the leaves was in the same range. TF value for Si significantly increased in response to exogenous Si application in the absence of Zn excess.

Zn excess increased Fe concentration in the roots but decreased it in the leaves (Table 3). Exogenous Si in the presence of Zn excess did not mitigate this trend and even decreased Fe concentration in the stem. Zn excess also increased Mg concentration in the roots and in the stem and slightly decreased it in the leaves. The highest leaf Mg content was recorded for CSi-treated plants and the lowest

Table 2 Zinc (Zn) and silicon (Si) concentrations and translocation factor (TF) in roots, stem, and leaves of *Cannabis sativa* (cv. Santhica 27)

	C	CSi	Zn	ZnSi
Zn (mg kg^{-1} DW)				
Roots	464 ± 172 *c*	280 ± 14 *c*	13,231 ± 236 *a*	11,110 ± 619 *b*
Stems	41 ± 2 *c*	52 ± 9 *c*	1362 ± 95 *a*	1035 ± 36 *b*
Leaves	57 ± 6 *c*	62 ± 4 *c*	1003 ± 31 *a*	904 ± 41 *b*
TF_c	0.11 ± 0.02 *b*	0.21 ± 0.05 *a*	0.08 ± 0.03 *b*	0.09 ± 0.06 *b*
	0.60 ± 0.12 *b*	1.17 ± 0.18 *a*	0.45 ± 0.15 *b*	0.55 ± 0.31 *b*
BF	294 ± 24.98 *a*	157 ± 6.59 *b*	49.95 ± 13.28 *c*	44.45 ± 9.42 *c*
Si (mg kg^{-1} DW)				
Roots	827 ± 38 *d*	3017 ± 101 *b*	945 ± 8 *c*	6948 ± 596 *a*
Stems	103 ± 34 *ab*	174 ± 4 *a*	55 ± 3 *b*	136 ± 21 *a*
Leaves	260 ± 4 *c*	3006 ± 116 *a*	162 ± 5 *d*	1941 ± 100 *b*
TF_c	0.26 ± 0.04 *b*	0.77 ± 0.19 *a*	0.15 ± 0.06 *c*	0.20 ± 0.04 *bc*
TF_a	1.41 ± 0.30 *b*	4.22 ± 0.77 *a*	0.79 ± 0.28 *c*	1.24 ± 0.42 *bc*
BF	0	6.20 ± 0.38 *a*	0	6.03 ± 0.61 *a*

Plants were exposed for 1 week to Zn (100 µM) in the presence or in the absence of 2 mM H_2SiO_3. *TFc*, translocation factor estimated on a concentration basis; TF_a, translocation factor estimated on a total amount basis. For a given parameter and a given organ, means followed by different letters are significantly different at $P < 0.05$ according to Tukey's HSD all-pairwise comparisons. Each value is the mean of 3 replicates

Table 3 Iron (Fe), magnesium (Mg), and sulfur (S) concentrations in roots, stem, and leaves of *Cannabis sativa* (cv. Santhica 27)

	C	CSi	Zn	ZnSi
Fe (mg kg^{-1} DW)				
Roots	1526 ± 37 *b*	922 ± 11 *c*	2281 ± 12 *a*	2298 ± 36 *a*
Stems	55 ± 4 a	42 ± 14 *ab*	58 ± 1 *a*	22 ± 4 *b*
Leaves	109 ± 4 *a*	115 ± 1 *a*	64 ± 2 *b*	55 ± 3 *b*
Mg (mg kg^{-1} DW)				
Roots	3537 ± 193 *c*	3346 ± 11 *c*	6631 ± 24 *a*	4754 ± 3 *b*
Stems	1295 ± 58 *b*	1639 ± 4 *a*	1599 ± 5 *a*	1419 ± 55 *b*
Leaves	4441 ± 12 *b*	5572 ± 5 *a*	4209 ± 31 *c*	3637 ± 83 *d*
S (mg kg^{-1} DW)				
Roots	2145 ± 205 *c*	2420 ± 107 *bc*	3963 ± 47 *a*	2897 ± 7 *b*
Stems	729 ± 12 *c*	1028 ± 77 *b*	1330 ± 52 *a*	746 ± 11 *c*
Leaves	1016 ± 126 *d*	1721 ± 1 *a*	1597 ± 115 *b*	1242 ± 14 *c*

Plants were exposed for 1 week to Zn (100 µM) in the presence or in the absence of 2 mM H_2SiO_3. For a given parameter and a given organ, means followed by different letters are significantly different at $P < 0.05$ according to Tukey's HSD all-pairwise comparisons. Each value is the mean of 3 replicates

for ZnSi-exposed ones. Exogenous Si in the absence of Zn excess increased S concentration in all organs. A similar effect was observed when plants were exposed to Zn excess in the absence of Si and was even more marked. In ZnSi-treated plants, S concentration increased in the roots and to a lower extent in the leaves but remained unmodified in the stem comparatively to control plants.

Photosynthesis-related Sparameters

In the absence of additional Si, Zn treatment had no impact on *Fv/Fm*, Φ_{PSII}, q_P, and NPQ values (Table 4). Similarly, it did not affect stomatal conductance (g_S), net photosynthesis (*A*), and instantaneous evapotranspiration (*E*) and intercellular CO_2 concentration (*Ci*). In the presence of additional Si, however, Zn significantly decreased Φ_{PSII}, q_P, g_s, and *E* values (Table 4). In the absence of Zn excess, exogenous Si surprisingly decreased Chl a, Chl b, and carotenoid content (Fig. 3). In the absence of Si, Zn excess decreased Chl a and carotenoids but had no impact on Chl b. Exogenous Si did not significantly mitigate the deleterious effect of Zn on these parameters.

Plant water and oxidative status

Water status was assessed using the osmotic potential (Ψ_S) and the water content (WC) of the leaves. As shown in Table 1, Zn in the absence of H_2SiO_3 significantly lowered Ψ_S values in leaves, while plants of the ZnSi treatment have similar values than control ones. WC was not affected by the applied treatments.

Malondialdehyde (MDA) is a cytotoxic product resulting from lipid peroxidation and commonly considered an indicator of oxidative stress. Its concentration increased in roots but remained unaffected in leaves of Zn-exposed plants compared to the controls (Fig. 4). The addition of Si significantly decreased MDA concentration in leaves of all treatments. In roots, Si application increased MDA concentration of plants cultivated in the absence of Zn excess.

Data for total antioxidant capacity for the hydrophobic (AOAD) and hydrophilic (AOAM) fractions are provided in Fig. 5. AOAD and AOAM fractions were reduced in plants exposed to Zn but increased when exposed to Si in the presence or absence of Zn excess.

Zn exposure strongly increased total glutathioneS (GSHt, Table 5) content in roots and leaves. The addition of silicon significantly decreased GSHt in roots and leaves of plants exposed to Zn, but also in leaves of plants cultivated in the absence of Zn excess. The ratio between oxidized (GSSG) and reduced glutathione (GSH) is an indicator of the oxidative stress undergone. GSSG/GSH ratio was significantly lower in roots and higher in leaves of Zn-treated plants compare to controls (Table 5). H_2SiO_3 application decreased GSSG/GSH in roots in the absence of Zn excess and increased this ratio in leaves of plants exposed to Zn.

Table 4 Photosynthesis-related parameters of *Cannabis sativa* (cv. Santhica 27)

	C	CSi	Zn	ZnSi
F_v/F_m	0.88 ± 0.03 *ab*	0.88 ± 0.01 *a*	0.85 ± 0.03 *b*	0.86 ± 0.01 *ab*
ϕ_{PSII}	0.83 ± 0.01 *a*	0.83 ± 0.03 *a*	0.80 ± 0.04 *ab*	0.74 ± 0.08 *b*
q_P	0.96 ± 0.02 *a*	0.97 ± 0.01 *a*	0.96 ± 0.02 *ab*	0.89 ± 0.08 *b*
NPQ	0.16 ± 0.04 *a*	0.16 ± 0.03 *a*	0.15 ± 0.03 *a*	0.24 ± 0.11 *a*
g_s (mmol m^{-2} s^{-1})	745 ± 565 ab	1012 ± 729 *a*	301 ± 186 *bc*	205 ± 163 *c*
A (µmol m^{-2} s^{-1})	2.44 ± 2.07 *a*	2.67 ± 1.35 *a*	1.57 ± 1.49 *a*	2.23 ± 1.09 *a*
E (mmol m^{-2} s^{-1})	2.95 ± 0.80 *ab*	3.22 ± 0.56 a	1.72 ± 1.01 *bc*	1.62 ± 1.16 *c*
C_i (µmol mol^{-1})	402 ± 24 *a*	406 ± 16 *a*	415 ± 15 *a*	385 ± 32 *a*

Plants were exposed for 1 week to Zn (100 µM) in the presence or in the absence of 2 mM H_2SiO_3. Maximum quantum yield of dark acclimated leaves (F_v/F_m), the photochemical efficiency of photosystem II (Φ_{PSII}), photochemical quenching (q_P), non-photochemical quenching (NPQ), stomatal conductance (g_s), net photosynthesis (*A*), instantaneous evapotranspiration (*E*), CO_2 in intercellular spaces (C_i). For a given organ, different letters indicate significant differences at $P < 0.05$. Each value is the mean of 5 replicates

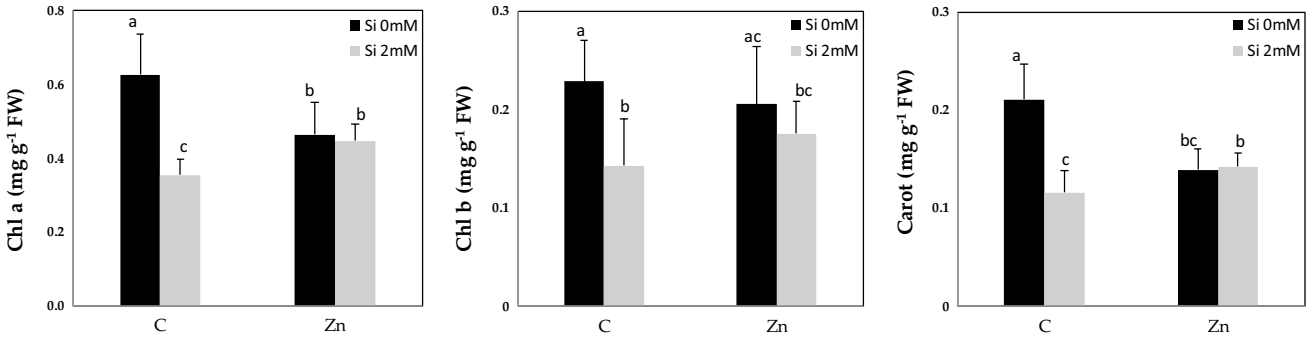

Fig. 3 Chlorophyll (**a**, **b**) and carotenoid content of *Cannabis sativa* (cv. Santhica 27) exposed for 1 week to Zn (100 µM), in the presence or in the absence of 2 mM H_2SiO_3. Data are means ± standard errors ($n = 5$). Values with different letters are significantly different ($P < 0.05$; Tukey's HSD all-pairwise comparisons)

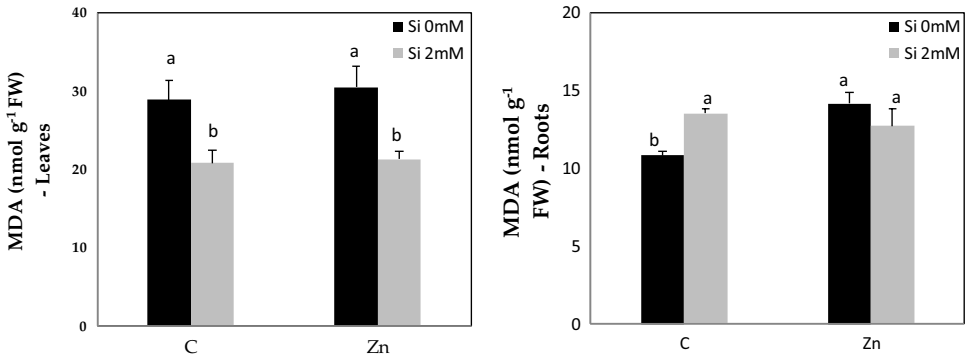

Fig. 4 Malondialdehyde (MDA) content in leaves and roots of *Cannabis sativa* (cv. Santhica 27) exposed for 1 week to Zn (100 µM), in the presence or in the absence of 2 mM H_2SiO_3. Data are means ± standard errors ($n = 5$). Values with different letters are significantly different ($P < 0.05$; Tukey's HSD all-pairwise comparisons)

As far as roots are concerned, PC concentration was significantly higher in ZnSi-treated plants than in CSi-exposed ones. Zn in the absence of Si had no effect on root PC concentration. PC was higher in the leaves than in the roots for all treatments: the highest value was recorded for plants exposed to Zn in the absence of Si, since exogenous Si significantly reduced the PC concentration of Zn-treated plants.

Discussion

The present study confirmed that Zn significantly accumulated in *C. sativa* cultivated in nutrient solution under Zn excess. However, growth properties were only marginally affected by Zn excess: only the total leaf number and stem length were reduced after 1 week of exposure to 100 µM

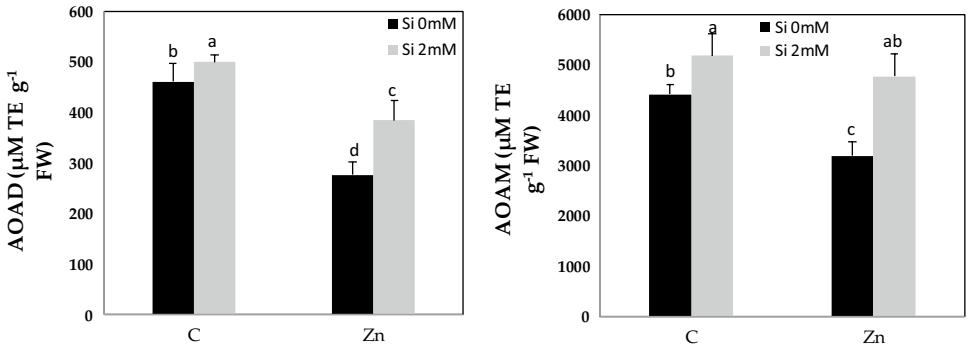

Fig. 5 Total antioxidant activity in the hydrophobic fraction (AOAD) and the hydrophilic fraction (AOAM) of leaves of *Cannabis sativa* (cv. Santhica 27). Plants were exposed for 1 week to Zn (100 µM), in the presence or in the absence of 2 mM H_2SiO_3. Data are means ± standard errors ($n = 5$). Values with different letters are significantly different ($P < 0.05$; Tukey's HSD all-pairwise comparisons)

Table 5 Total glutathione (GSHt), oxidize (GSSG)/reduced (GSH) glutathione, and phytochelatine (PC) concentrations in roots and leaves of *Cannabis sativa* (cv. Santhica 27)

	C	CSi	Zn	ZnSi
Roots				
GSHt (nmol g^{-1} FW)	176 ± 20 *c*	82 ± 34 *d*	1622 ± 171 *a*	762 ± 37 *b*
GSSG/GSH	14.38 ± 6.85 *a*	5.89 ± 5.84 *b*	3.61 ± 0.73 *b*	8.43 ± 4.27 *ab*
PC (nmol g^{-1} FW)	241 ± 28 *ab*	209 ± 20 *b*	222 ± 37 *ab*	275 ± 55 *a*
Leaves				
GSHt (nmol g^{-1} FW)	412 ± 19 *c*	294 ± 33 *d*	824 ± 161 *a*	564 ± 48 *b*
GSSG/GSH	6.03 ± 0.27 *c*	7.07 ± 0.76 *c*	11.12 ± 2.28 *b*	14.56 ± 1.70 *a*
PC (nmol g^{-1} FW)	821 ± 84 *c*	658 ± 24 *d*	1243 ± 73 *c*	974 ± 121 *b*

Plants were exposed for 1 week to Zn (100 µM) in the presence or in the absence of 2 mM H_2SiO_3. Maximum quantum yield of dark acclimated leaves (F_v/F_m), the photochemical efficiency of photosystem II (Φ_{PSII}), photochemical quenching (q_P), non-photochemical quenching (NPQ), stomatal conductance (g_s), net photosynthesis (A), instantaneous evapotranspiration (E), CO_2 in intercellular spaces (C_i). For a given organ, different letters indicate significant differences at $P < 0.05$. Each value is the mean of 5 replicates

Zn while both fresh and dry weights remained unchanged. This suggests that hemp is able, to some extent, to display resistance mechanisms to toxic Zn doses.

In plants exposed to Zn excess, Zn concentration in the stem was higher than in the leaves. This could be linked to the fixing properties of the fibers which are exploited for biosorption purposes by numerous authors (Pejic et al. 2009; Vukcevic et al. 2014a, 2014b). Zinc is indeed able to bind to carboxyl and hydroxyl groups of cell wall polymers such as those occurring in bast fibers, and Loiacono et al. (2018) recently demonstrated that hemp fibers may be efficiently used to clean up waste water contaminated by numerous HM. Wall retention could also occur *in planta*, during the formation of the fibers, although this implies that HM need to be in close contact with the fiber while bast fibers are located in the phloem rather than in the xylem where transpiration stream occurs.

Zn translocation from roots to shoots, estimated on a concentration basis (TF_c), was however limited ($TF_c \sim 0.1$) but it could also be interesting to estimate TF on a total amount basis (TF_a, Table 3) based on the quantities actually exported from the substrate (Ali et al. 2013). For all treatments, translocation factor estimated on a total amount basis (TF_a) was higher than translocation factor estimated on a concentration basis (TF_c) but always remained lower than 1. This suggests that, despite a good level of tolerance, hemp adopted an excluding strategy. A similar observation has already been reported by Angelova et al. (2004), Löser et al. (2002), and Shi et al. (2009) in hemp exposed to HM. Root sequestration is a strategy widely developed by non-hyperaccumulating plants to avoid the accumulation of toxic elements in photosynthetic tissues (Ali et al. 2013; Kanwar et al. 2020).

Despite root sequestration attempt, we demonstrated that Zn may accumulate up to 1 $g.Kg^{-1}$ DW in hemp leaves. Such a level of accumulation had only a marginal impact on photosynthesis-related parameters. Chlorophyll a and carotenoids were indeed the only parameters reduced by Zn. Piotrowska-Cyplik and Czarnecki (2003) and Linger et al. (2005) suggested that on a long-term basis, a reduction of pigment content, and therefore in the availability of photoassimilats, may explain the reduced biomass production in

hemp. The present work however suggests that on a short-term basis, photosynthesis is resilient to Zn toxicity in *Cannabis sativa* since the decrease in photosynthetic pigments had no impact on net photosynthesis. Zinc was reported to substitute to Mg within chlorophyll (Küpper et al. 1998) and in Rubisco (Cambrollé et al. 2013) but in the present study, Zn excess reduced the leaf Mg concentration by 5.2% only (Table 3) making this substitution unlikely. Water content was not affected by the treatments applied but Zn excess significantly lowered Ψ_S values in leaves, which is a clear indication that adaptations were required for Zn-treated plants to maintain internal water potential and turgor. Such accumulation of osmotic compounds contributes to turgor maintenance and CO_2 diffusion within the mesophyll. This probably explain stable *C*i values in plants exposed to Zn excess compare to controls.

The present study also showed that hemp exposed to Zn excess encountered a moderate oxidative stress: MDA content in leaves remained similar to controls but increased in roots. Zinc accumulated to higher amounts in the roots than in the leaves; hence, a higher oxidative stress in the below part of the plant was not unexpected. This suggests that ROS were quickly scavenged in leaves. Reduced glutathione (GSH) is involved in the reduction of an important part of ROS generated by stress (Shahid et al. 2019). In our study, Zn exposure led to higher leaf GSHt concentration and GSSG/GSH ratio, suggesting that GSH helped to withstand oxidative stress in leaves. This may also explain the decrease of total antioxidant capacity, GSH being part of the AOAM fraction. Besides its role as an antioxidant, GSH acts as a precursor of phytochelatin (PC) synthesis. In our study, Zn exposure increased PC content in the leaves but not in the roots. Chelating metals by forming PCs or metallothioneins (MTs) metal complexes at the intra- and intercellular level are part of the mechanisms used by plants to counteract HM toxicity (Citterio et al., 2003; Tennstedt et al. 2009; Emamverdian et al., 2015). Nevertheless, a higher PC concentration in the leaves than in the roots is rare in plants exposed to Zn. In plants facing ion toxicities, the first priority is to protect the photosynthetic machinery (Muthusaravanan et al. 2018). We demonstrated that on a short-term basis, hemp is perfectly able to trigger PC oversynthesis as an emergency strategy to protect photosynthetic tissues and the recorded increase in leaf S concentration is in line with this hypothesis. We recently showed in another study that 1-week exposure to 100 µM Zn upregulated the expression of a gene coding for phytochelatin synthase (*PCS1*) in *Cannabis sativa* (Luyckx et al. 2021c). The major drawback of PC synthesis is that it requires a lot of energy and has a high metabolic cost (Khan et al. 2000; Kanwar et al. 2020; Kurade et al. 2021). This might explain that plants exposed to Zn for longer duration improve root sequestration mechanisms and reduce the need for PC synthesis in the leaves (Emamverdian et al. 2015; Lefèvre et al. 2016).

Although Si is not considered essential for plants, it intervenes as a beneficial element in their defense and growth. Hemp is not considered an Si accumulator under normal conditions. However, in this study, control plants maintained in nutrient solution contained Si in similar range than plants grown in non-polluted soils (Epstein 1994; Luyckx et al. 2019). Additional Si significantly increased root and leaf Si concentration in the absence and in the presence of Zn excess. In roots, plants of CSi treatment accumulated 3.6 × more Si than plants of C treatment while ZnSi-treated plants accumulated 7.4 × more Si than plants of Zn treatment. This suggests that plants stimulated Si uptake to cope with Zn stress. In rice exposed to heavy metals and Si, Kim et al. (2017) and Ma et al. (2015) reported an increase in the expression of genes involved in the transport of Si (*OsLSi1* and *OsLSi2*) to improve resistance to metal stress. Similarly, Luyckx et al. (2021c) reported that the expression of *Lsi2-1* in hemp roots was increased after 1-week exposure to 100 µM Zn. In the present case, however, high Si accumulation in the root of ZnSi-treated plants did not protect the roots from oxidative stress since MDA concentration was similar in ZnSi- and Zn-treated plants.

H_2SiO_3 application under Zn exposure interfered with Zn absorption. Zn concentration was clearly lower in roots, stems, and leaves of Si-treated plants in the presence of Zn excess than in plants exposed to Zn in the absence of Si. A first hypothesis is that the presence of Si in the nutrient solution reduces Zn availability through the precipitation of Zn silicate. Bokor et al. (2014) indeed mentioned that Zn_2SiO_4 may occur in water experiments, but this is not confirmed by the speciation program VISUAL MinTEQ which clearly indicated that, for the range of concentration and pH of the solution used in our study, Zn remained fully soluble in the solution. The decrease of Zn concentration cannot be attributed to a decrease in transpiration rate since no significant difference for *E* values was observed between ZnSi and Zn treatments. It has already been observed in rice plants treated with Cu/Cd a decrease in the expression of HM transporters in the presence of Si (Kim et al. 2017; Ma et al. 2015). Huang and Ma (2020) recently demonstrated in rice that Si supply decreased Zn concentration in both the root and the shoots: according to these authors, Si acts on Zn uptake by downregulating *OsZIP1* implicated in Zn uptake. The comparison should however be established with caution considering that rice is a specific plant species for Si hyperaccumulation and that data obtained with rice are not necessarily valid for other plant species, especially dicots. Beside Zn absorption, some authors reported that Si may reduce Zn translocation from the root to the shoot (Zajaczkowska et al. 2020) but this was not observed in our experiment since TF value for Zn was hardly modified by Si. This

implies that as far as hemp is concerned, Si may impact transporters involved in Zn uptake (especially those encoded by *ZIP* genes) but had no impact on transporters involved in Zn xylem loading and long-distance transport (HMA2 and HMA4) (Zlobin 2021).

Exogenous application of Si under Zn excess increased total antioxidant capacity (AOAM and AOAD fractions) and decreased MDA content mainly in the leaves, as already observed by Kim et al. (2017). This suggests that Si may trigger oxidative tolerance processes in hemp. The same beneficial effect of Si was noticed in leaves of control plants. Increased antioxidant capacity under Si exposure suggested a higher GSHt content. However, in the present study, GSHt content decreased following Si application under Zn excess. The increase in the antioxidant capacity despite a decrease in GSHt content may be due to activation of other antioxidants by Si: the fact that both AOAD and AOAM antioxidant activities increased in response to Si suggests indeed that other compounds, such as ascorbate and α-tocopherol, which were not quantified in the present study, may increase in response to exogenous Si. Moreover, the lower Zn accumulation induced by Si probably contributed to decrease ROS production and the need of GSH as an antioxidant and as a precursor of PC synthesis. PC content in leaves was indeed decreased in plants of ZnSi treatment comparatively to Zn-treated plants, while we observed an opposite trend in roots, although Si decreased Zn accumulation in both organs. This suggests that PC more efficiently sequester Zn in the leaves than in the roots: while Zn concentrations in the roots are quite high, PC contents were unexpectedly low. Using K-edge extended X-ray absorption fine structure (EXAFS) spectroscopy measurements, Lefèvre et al. (2016) demonstrated that in the roots of HM resistant species *Zygophyllum fabago*, Zn mainly coordinate to Zn–O/N–C groups suggesting that PC did not play a key role in Zn tolerance in this organ and that other compounds, such as organic acid or polyamines, may be involved.

As a matter of fact, exogenous Si provides some metabolic advantages to hemp exposed to Zn excess, especially in relation to a decrease in Zn accumulation in the different parts of the plant. However, this was not sufficient to significantly increase plant growth on a short-term basis. Bokor et al. (2014) found similar data regarding maize cultivars simultaneously exposed to Zn and Si. According to these authors, increasing concentration of Si in combination with Zn treatment even increased physiological stress in comparison to Zn treatment. Similar results were observed by Masarovic et al. (2012) who observed no positive effects of Si on sorghum exposed to high Zn concentrations in the medium.

Conclusion

Young plants of *Cannabis sativa* cv Santhica cultivated in nutrient solution were able to cope with 100 µM Zn during a short-term (1 week) exposure. Zinc excess did not induce plant mortality and only marginally affected plant growth. Hemp accumulated high amounts of Zn, with a preferential location at the root level. Zinc accumulation in the leaves had no impact on photosynthetic properties, except a decrease in chlorophyll a and carotenoid content. Photosynthesis resilience may be due to over-synthesis of phytochelatins sequestering Zn excess in the leaves and to the increase in endogenous antioxidant protecting photosynthetic tissues from oxidative stress. Exogenous Si decreased Zn concentrations in all organs and increased total antioxidant content. Si was however unable to significantly improve the growth of stressed plants. Hemp thus appears as a promising species to valorise Zn-polluted agricultural soils and Si may provide physiological advantages to stressed plants. Additional researches using longer-time exposures are required to precise more extensively the interest of hemp in phytoextraction and/or phytostabilization strategies.

Author contribution ML, GG, and SL designed the methodology; ML performed the whole experiment, treated and analyzed the data; JFH and SL supervised the whole research process; ML and SL wrote the original draft. All authors reviewed the manuscript.

Funding This work was financed by the ADEME (Agence de la Transition écologique; Convention MisChar no. 1672C0044), by the FNRS (Fonds National pour la Recherche Scientifique, convention no. T.0147.21), and by the Luxembourg National Research Fund (20/15045745).

Data availability All data generated or analyzed during this study are included in this published article.

Declarations

Ethics approval and consent to participate Not applicable.

Consent for publication. Not applicable.

Competing interests The authors declare no competing interests.

References

Adrees M, Ali S, Rizwan M, Zia-ur-Rehman M, Ibrahim M, Abbas F, Farid M, Qayyum MF, Irshad MK (2015) Mechanisms of silicon-mediated alleviation of heavy metal toxicity in plants: a review. Ecotox Environ Saf 119:186–197

Ahmad R, Tehsin Z, Malik ST, Asad SA, Shahza M, Bila M, Shah MM, Khan SA (2016) Phytoremediation potential of hemp (Cannabis sativa L.): identification and characterization of heavy metals responsive genes. CLEAN–Soil Air Water 44:195–201

Ali H, Khan E, Anwar Sajad M (2013) Phytoremediation of heavy metals — concepts and applications. Chemosphere 91:869–881

Alloway BJ (2013) Bioavailability of elements in soil. Essentials of Medical Geology, revised. Springer, Dordrecht, pp 351–373

Andrejić G, Gajić G, Prica M, Dželetovic Ž, Rakić T (2018) Zinc accumulation, photosynthetic gas exchange, and chlorophyll a fluorescence in Zn-stressed Miscanthus x giganteus plants. Photosynthetica 56:1249–1258

Angelova V, Ivanova R, Delibaltova V, Ivanov K (2004) Bio-accumulation and distribution of heavy metals in fibre crops (flax, cotton and hemp). Ind Crops Prod 19:197–205

Benzie IF, Strain JJ (1996) The ferric reducing ability of plasma (FRAP) as a measure of "antioxidant power": the FRAP assay. Anal Biochem 239:70–76

Berni R, Mandlik R, Hausman JF, Guerriero G (2021) Silicon-induced mitigatory effects in salt-stressed hemp leaves. Physiol Plant 171:476–482

Bokor B, Vaculík M, Slováková L, Masarovič D, Lux A (2014) Silicon does not always mitigate zinc toxicity in maize. Acta Physiol Plant 36:733–743

Bona E, Marsano F, Cavaletto M, Berta G (2007) Proteomic characterization of copper stress response in Cannabis sativa roots. Proteomics 7:1121–1130

Branda F, Malucelli G, Durante M, Piccolo A, Mazzei P, Costantini A, Silvestri B, Pennetta M, Bifulco A (2016) Silica treatments: a fire-retardant strategy or hemp fabric/epoxy composites. Polymers 8:313

Cambrollé J, Mancilla-Layton JM, Munoz-Vallès S, Figueuero-Luque E, Luque T, Figueuero-Luque ME (2013) Evaluation of Zn tolerance and accumulation potentiel of the coastal shrub Limoniastrum monopetalum (L.) Boiss. Environ Exp Bot 85:50–57

Cereser C, Guichard J, Drai J, Bannier E, Garcia I, Boget S, Parvaz P, Revol A (2001) Quantitation of reduced and total glutathione at the femtomole level by high-performance liquid chromatography with fluorescence detection: application to red blood cells and cultured fibroblasts. J Chrom b: Biomedical Sci Appl 752:123–132

Citterio S, Santagostino A, Fumagalli P, Prato N, Ranalli P, Sgorbati S (2003) Heavy metal tolerance and accumulation of Cd, Cr and Ni by Cannabis sativa L. Plant Soil 256:243–252

De Vos CR, Vonk MJ, Vooijs R, Schat H (1992) Glutathione depletion due to copper-induced phytochelatin synthesis causes oxidative stress in Silene cucubalus. Plant Physiol 98:853–858

Deleuran LC, Flengmark PK (2006) Yield potential of hemp (Cannabis sativa L.) cultivars in Denmark. J Ind Hemp 10:19–31

Doncheva S, Poschenrieder C, Stoyanova Z, Georgieva K, Velichkova M, Barceló J (2009) Silicon amelioration of manganese toxicity in Mn-sensitive and Mn-tolerant maize varieties. Environ Exp Bot 65:189–197

Dufey I, Gheysens S, Ingabire A, Lutts S, Bertin P (2014) Silicon application in cultivated rice (Oryza sativa L. and O. glaberrima Steud.) alleviates iron toxicity symptoms through the reduction in iron concentration in the leaf tissue. J Agron Crop Sci 200:132–142

Emamverdian A, Ding Y, Mokhberdoran F, Xie Y (2015) Heavy metal stress and some mechanisms of plant defense response. Sci World J 2015:756120

Epstein E (1994) The anomaly of silicon in plant biology. Proc Nat Acad Sci USA 91:11–17

Etesami H, Jeong BR (2018) Silicon (Si): review and future prospects on the action mechanisms in alleviating biotic and abiotic stresses in plants. Ecotox Environ Saf 147:881–896

Fan W, Guo Q, Liu CY, Liu X, Zhang M, Long D, Xiang Z, Zhao A (2018) Two mulberry phytochelatin synthase genes confer zinc/cadmium tolerance and accumulation in transgenic Arabidopsis and tobacco. Gene 645:95–104

Goodarzi A, Namdjoyan S, Soorki AA (2020) Effects of exogenous melatonin and glutathione on zinc toxicity in safflower (Carthamus tinctorius L.) seedlings. Ecotox Environ Saf 201:110853

Heath RL, Packer L (1968) Photoperoxidation in isolated chloroplasts: II. Role of electron transfer. Arch Biochem Biophys 125:850–857

Huang S, Ma JF (2020) Silicon suppresses zinc uptake through down-regulating zinc transporter gene in rice. Phyiol Plant 170:580–591

Imtiaz M, Rizwan MS, Mushtag MA, Ashraf M, Shahazad SM, Yousaf B, Saeed DA, Rizwan M, Nawaz MA, Mehmood S, Tu S (2016) Silicon occurrence, uptake, transport and mechanisms of heavy metals, minerals and salinity enhanced tolerance in plants with future prospects: a review. J Env Manag 183:521–529

Jiang Y, Bourebrab MA, Sid N, Taylor A, Collet F, Pretot S, Hussain A, Ansell M, Lawrence M (2018) Improvement of water resistance of hemp woody substrates through deposition of functionalized silica hydrophobic coating while retaining excellent moisture buffering properties. Sus Chem Eng 6:10151–10161

Kanwar VS, Sharma A, Srivastav AL, Ranni L (2020) Phytoremediation of toxic metals present in soil and water environment: a critical review. Environ Sci Poll Res 27:44835–44860

Khan AG, Kuek C, Chaudhry TM, Khoo CS, Hayes WJ (2000) Role of plants, mycorrhizae and phytochelators in heavy metal contaminated land remediation. Chemosphere 41:197–207

Kim YH, Khan AL, Waqas M, Lee IJ (2017) Silicon regulates antioxidant activities of crop plants under abiotic-induced oxidative stress: a review. Front Plant Sci 8:510

Kröger N, Poulsen N (2008) Diatoms – from cell wall biogenesis to nanotechnology. Ann Rev Genet 42:83–107

Kumar S, Singh R, Kumar V, Rani A, Jain R (2017) Cannabis sativa: A plant suitable for phytoremediation and bioenergy production. Phytoremediation potential of bioenergy plants. Springer, Singapore, pp 269–285

Küpper H, Küpper F, Spiller M (1998) In situ detection of heavy metal substituted chlorophylls in water plants. Photosynth Res 58:123–133

Kurade MMB, Ha YH, Xiong JQ, Govindar SP, Jang M, Jeon BH (2021) Phytoremediation as a green biotechnology tool for emerging environmental pollution: a step towards sustainable rehabilitation of the environment. Chem Eng J 415:129040

Lefèvre I, Vogel-Mikuš K, Arčon I, Lutts S (2016) How do roots of the metal-resistant perennial bush Zygophyllum fabago cope with cadmium and zinc toxicities? Plant Soil 404:193–207

Lichtenthaler HK (1987) Chlorophylls and carotenoids - pigments of photosynthetic biomembranes. Meth Enzymol 148:350–382

Linger P, Müssigg J, Fischer H, Kobert J (2002) Industrial hemp (Cannabis sativa L.) growing on heavy metal contaminated soil: fibre quality and phytoremediation potential. Ind Crops Prod 16:33–42

Linger P, Ostwald A, Haensler J (2005) Cannabis sativa L. growing on heavy metal contaminated soil: growth, cadmium uptake and photosynthesis. Biol Plant 49:567–576

Liu L, Li W, Song W, Guo M (2018) Remediation techniques for heavy metal-contaminated soils: principles and applicability. Sci Total Enviro 633:206–219

Loiacono S, Morin-Crini N, Martel B, Chanet G, Bradu C, Torri G, Crini G (2018) Complexation du zinc, du cuivre et du manganese par du chanvre: efficacité chimique et impact écotoxicologique. Environ Risques Santé 17:240–252

Löser C, Zehnsdorf A, Fussy A, Stärk HJ (2002) Conditioning of heavy metal-polluted river sediment by Cannabis sativa L. Intern J Phytorem 4:27–45

Luo Y, Zheng Z, Wu P, Wu Y (2022) Effect of different direct revegetation strategies in the mobility of heavy metals in artificial smelting waste slag: implications for phytoremediation. Chemosphere 286:131678

Luyckx M, Berni R, Cai G, Lutts S, Guerriero G (2019) Impact of heavy metals on non-food herbaceous crops and prophylactic role of Si. Plant Metallomics and Functional Omics. Springer, Cham, pp 303–321

Luyckx M, Hausman JF, Blanquet M, Guerriero G, Lutts S (2021) Silicon reduces cadmium absorption and increases root-to-shoot translocation without impacting growth in young plants o hemp (*Cannabis sativa* L.) on a short- term basis. Environ Sci Poll Res 28:37963–37977

Luyckx M, Hausman JF, Isenborgh A, Guerriero G, Lutts S (2021) Impact of cadmium and zinc on proteins and cell wall-related

gene expression in young stems of hemp (Cannabis sativa L.) and influence of exogenous silicon. Environ Exp Bot 183:104363
Luyckx M, Hausman JF, Sergeant K, Guerriero G, Lutts S (2021) Molecular and biochemical insights into early responses of hemp to Cd and Zn exposure and the potential effect of Si on stress response. Front Plant Sc 12:711853
Ma J, Cai J, He C, Zhang W, Wang L (2015) A hemicellulose-bound form of silicon inhibits cadmium ion uptake in rice (Oryza sativa) cells. New Phytol 206:1063–1074
Masarovic D, Slováková L, Bokor B, Budjoš M, Lux A (2012) Effect of silicon application in Sorghum bicolor exposed to toxic concentration of zinc. Biologia 67:706–717
Maxwell K, Johnson GN (2000) Chlorophyll fluorescence – a practical guide. J Exp Bot 51:659–668
Muthusaravanan S, Sivarajasekar N, Vivek JS, Paramasivan T, Naushad M, Prakashmaran J, Gayathri V, Al-Duaij OK (2018) Phytoremediation of heavy metals: mechanisms, methods and enhancements. Environ Chem Lett 16:1339–1359
Pejic B, Vukcevic M, Kostic M, Skundric P (2009) Biosorption of heavy metal ions from aqueous solutions by short hemp fibers: effect of chemical composition. J Hazard Mat 164:146–153
Piotrowska-Cyplik A, Czarnecki Z (2003) Phytoextraction of heavy metals by hemp during anaerobic sewage sludge management in the non-industrial sites. Pol J Environ Stud 12:779–784
Schäfer HJ, Greiner S, Rausch T, Haag-Kerwer A (1997) In seedlings of the heavy metal accumulator Brassica juncea, Cu^{2+} differentially affects transcript amounts for γ-glutamylcysteine synthetase (γ-ECS) and metallothionein (MT2). FEBS Lett 404:216–220
Schluttenhofer C, Yuan L (2017) Challenges towards revitalizing hemp: a multifaced crop. Trends Plant Sci 22:917–929
Shahid M, Khalid S, Abbas G, Niazi NK, Murtaza B, Rashid MI, Bibi I (2019) Redox mechanisms and plant tolerance under heavy metal stress: genes and regulatory networks. Plant Metallomics and Functional Omics. Springer, Cham, pp 71–105
Shi GR, Cai QS, Liu QQ, Wu L (2009) Salicylic acid-mediated alleviation of cadmium toxicity in hemp plants in relation to cadmium uptake, photosynthesis, and antioxidant enzymes. Acta Physiol Plant 3:969–977
Shi G, Liu C, Cui M, Ma Y, Cai Q (2012) Cadmium tolerance and bioaccumulation of 18 hemp accessions. Appl Biochem Biotechnol 168:163–173
Sun W, Liu S, Zhang X, Zhu H (2022) Performance of hyperspectral data in predicting and mapping zinc concentration in soil. Sci Total Environ 824:153766
Tennstedt P, Peisker D, Böttcher C, Trampczynska A, Clemens S (2009) Phytochelatin synthesis is essential for the detoxification of excess zinc and contributes significantly to the accumulation of zinc. Plant Physiol 149:938–948
Tóth G, Hermann T, Da Silva MR, Montanarella L (2016) Heavy metals in agricultural soils of the European Union with implications for food safety. Environ Intern 88:299–309
Vareda JP, Valente AJM, Durães L (2019) Assessment of heavy meal pollution from anthropogenic activities and remediation strategies: a review. J Environ Manag 246:101–1018
Vukcevic M, Pejic B, Kaliajadis A, Pajic-Lijakovic I, Kostic M, Lausevic Z, Lausevic M (2014) Carbon material from waste short hemp fibers as a sorbent for heavy metal ions – mathematical modeling of sorbent structure and ions transport. Chem Eng J 233:284–292
Vukcevic M, Pejic B, Lausevic M, Pajic-Lijaovic I, Kostic M (2014) Influence of chemically modified short hemp fiber structure on biosorption process of Zn^{2+} ions from waste water. Fib Pol 15:687–697
Wu Y, Trejo HX, Chen G, Li S (2021) Phytoremediation of contaminants of emerging concern from soil with industrial hemp (Cannabis sativa L.): a review. Environ Dev Sustain 23:14405–14435
Yang R, Berthold AC, McCurdy CR, da Silva BS, Brym ZT, Freeman JH (2020) Development of cannabinoids in flowers of industrial hemp (Cannabis sativa L.): a pilot study. J Agr Food Chem 68:6058–6064
Zajaczkowska A, Korzeniowska J, Sienkiewicz-Choleva U (2020) Effect of soil and foliar silicon application on the reduction of zinc toxicity in wheat. Agriculture 10:0522
Zhao J, Xu Y, Wang W, Griffin J, Roozeboom K, Wang D (2020) Bioconversion of industrial hemp biomass for bioethanol production: a review. Fuel 281:118725
Zlobin IE (2021) Current understanding of plant zinc homeostasis regulation mechanisms. Plant Physiol Biochem 162:327–335